ACS Combinatorial Science

Research Article

pubs.acs.org/acscombsci

Screening of Novel Li−Air Battery Catalyst Materials by a Thin Film Combinatorial Materials Approach

John G. Hauck and Paul J. McGinn*

Department of Chemical and Biomolecular Engineering, University of Notre Dame, Notre Dame, Indiana 46556, United States

Supporting Information

ABSTRACT: A combinatorial synthesis and high-throughput screening process was developed for the investigation of potential oxygen reduction reaction (ORR) and oxygen evolution reaction (OER) catalysts for use as Li−air battery cathode materials. Libraries of discrete ternary metal alloy compositions were deposited via thin-film sputtering. The samples were electrochemically tested in parallel using cyclic voltammetry in O_2-saturated KOH electrolyte. Compositions were ranked by ORR and OER onset potentials with respect to an internal Pt reference. Results from the Pt−Mn−Co, Cr−Mn−Co, Pd−Mn−Co, and Pd−Mn−Ru systems are reported. Many alloy compositions showed marked improvement in catalytic activity compared to pure Pt. Among the systems considered, $Pt_{12}Mn_{44}Co_{44}$, $Pd_{43}Co_{57}$ and $Pd_{36}Mn_{28}Ru_{36}$ in particular exhibited lower overpotentials for oxygen reactions, which occur at the cathode in Li−air batteries.

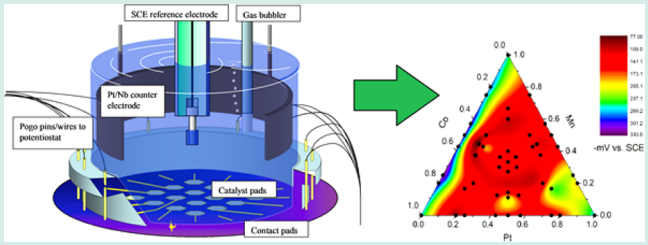

KEYWORDS: *combinatorial electrochemistry, Li−air battery, oxygen reduction, oxygen evolution, combinatorial sputtering*

INTRODUCTION

Because of the increasing power needs of small portable electronics, coupled with the desire for electric vehicles, there is demand for higher energy density and higher capacity batteries. For example, the current commercial battery Li−ion chemistry is not sufficient to meet the projected demands of a "500 mile" battery for the automotive industry. The Li-air battery offers great potential in this regard.[1−3] A Li−air battery consists of a Li metal anode and atmospheric oxygen cathode, separated by an electrolyte. The theoretical specific energy of this cell is 11 140 Wh/kg at 2.96 V cell voltage, which is much more powerful than Li−ion batteries on the market today.[4] However, there are many battery design challenges which lead to Li−air energy densities far smaller than the theoretical value. These are discussed in detail in several recent reviews.[5−8] The main source of polarization losses is in the cathode because of the sluggishness and high activation energy of the oxygen reduction reaction (ORR). This suggests the need for an ORR catalyst to facilitate higher reaction rates (higher current density) and less overpotential (higher cell voltage).[9,10] A catalyst is also required to promote the oxygen evolution reaction (OER) to reduce charging times and voltages.[11] Hence, a bifunctional catalyst would be ideal.

A number of potential ORR catalysts have been examined for Li−air battery application including graphite,[4] high surface area carbon,[12] carbon nanotubes,[13] Pt,[14] Au,[15] Pt−Au nanoparticles,[11] MnO_2,[16,17] and various metal oxide spinels and perovskites.[18−20] The catalysts that have typically been used for ORR and OER utilize precious metals, such as Pt (or Pt−Au for secondary batteries), which is not desirable for manufacture because of the high cost. A non-noble metal catalyst that exhibits the high catalytic activity of Pt−Au is greatly desired. Additionally, alloying Pt with other metals has the potential to increase catalyst performance because of the volcano effect caused by shifting the Pt d-band center, as has been shown in ORR studies for fuel cell electrocatalysts.[21] Another possible source of catalyst improvement is the formation of a Pt- or Pd-skin surface structure with an advantageous underlying electronic structure.[22] The present study aims to develop a protocol to identify potential Li−air battery catalyst materials by a combinatorial synthesis and high-throughput screening approach based on thin film deposition and characterization.

Combinatorial synthesis has over the past decade been applied in many fields of materials science including polymers, glasses, catalysts, dielectrics, and electronic and magnetic materials.[23−25] When combined with high-throughput characterization or screening techniques, it is a quick and efficient method to identify the optimum composition or processing schedule among many candidate compounds or conditions. Several research groups have reported different combinatorial procedures to study aspects of Li−ion battery development, including gradient thin films sputtered onto an electrode grid,[26] powder production through automated liquid handling,[27−30] scanning of a thin film electrode grid using a serial characterization probe,[31,32] and microfabrication of thin film batteries with solid-state electrolytes.[33] Most recently Jun et al. reported the use of optical screening approach to examine Pd-based alloys for use as cathode catalysts in Li−air batteries.[34]

Received: February 13, 2015
Revised: April 15, 2015
Published: May 12, 2015

DOI: 10.1021/acscombsci.5b00030
ACS Comb. Sci. 2015, 17, 355−364

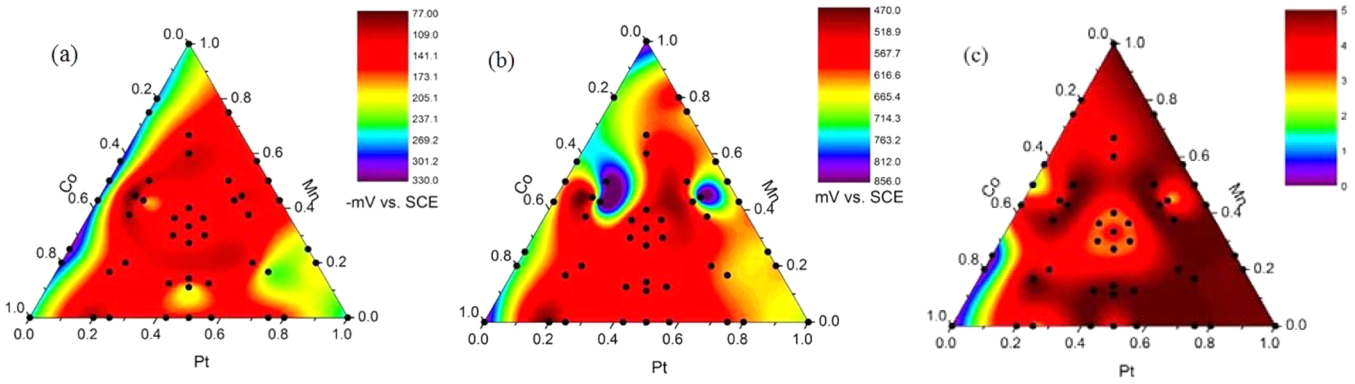

Figure 1. (a) ORR onset potentials for the Pt−Mn−Co system. (b) OER onset potentials for the Pt−Mn−Co system. (c) Corrosion scores for the Pt−Mn−Co system.

The ORR has been studied for decades and many catalyst materials and conditions have been examined, but few of these studies have been directed toward use in Li−air batteries. Two possible Li−air battery designs make use of an aqueous alkaline electrolyte and an aprotic organic solvent.[35,36] ORR in alkaline media has been studied in the context of the alkaline fuel cell, in which Pt is the most common catalyst, along with Pt−Co alloys.[37−41] Voltammetric studies can be used to determine catalyst effectiveness in alkaline media,[42] and voltammetric performance in an alkaline medium can be correlated to catalytic performance in a Li−air battery with aprotic organic electrolyte.[43]

Battery electrodes are typically in the form of composite thick films in which an electroactive powder is dispersed with carbon black in a binder. However, research into the electrochemical properties of active materials can be advantageously performed by studying thin films of the pure material, rather than the particulate or battery electrode form. Thin film approaches offer a high degree of composition and thickness control, and avoid issues such as particle size effects, dispersion issues, and compositional nonuniformity. Differences in catalytic activity among prospective compounds may be attributed solely to composition when in the thin film regime.[44]

This study describes the development and application of a thin film combinatorial synthesis and high-throughput screening method for Li−air cathode catalyst materials. Combinatorial synthesis was performed by sputter deposition of ternary libraries on Si substrates. High-throughput screening was accomplished using parallel cyclic voltammetry in a multielectrode electrochemical cell. Several compositional systems were scanned for ORR and OER catalytic activity in alkaline media, and promising compositions were identified for further study. Systems reported in this study include Pt−Mn−Co, Cr−Mn−Co, Pd−Mn−Co, and Pd−Mn−Ru.

RESULTS AND DISCUSSION

Pt was used as the reference material for catalytic activity toward ORR and OER for this study. Each library contained 12 Pt electrodes around the periphery as an internal reference for library compositions, as well as to allow for comparison of results between libraries. The ORR onset potential in KOH was found to be −220 mV vs SCE over many libraries tested. This is in good agreement with reports in the literature for Pt single crystals and carbon-dispersed nanoparticles in alkaline solutions.[45,46] The sputtered Pt films were crystalline, with primarily a (111) orientation, as determined by X-ray diffraction. Catalyst materials with higher ORR onset potentials than Pt are desirable, as well as less expensive catalysts that approach the Pt onset potential value. The OER onset potential was found to be 760 mV vs SCE over many libraries tested, which is also consistent with literature results for a Pt metal electrode.[47] Catalyst materials with lower OER onset potentials than Pt are desirable for secondary Li−air battery applications.

Pt−Mn−Co. The Pt−Mn−Co system was examined based on the known performance of Pt and Pt−Co alloys as ORR catalysts and the prior reports of the use of Mn compounds in Li−air batteries. Compositions of Pt−Mn−Co ternary alloys have also been investigated for ORR activity in recent studies.[48−50] These reports suggested specific low Mn alloys exhibited good ORR activity and durability in a fuel cell environment.

Pt−Mn−Co libraries were fabricated and tested using cyclic voltammetry as described above and were subsequently ranked for ORR and OER catalytic activity according to their onset potential. The onset potential rankings were projected onto ternary contour maps to identify activity trends with composition (Figure 1). In these maps, the point locations represent the ternary alloy composition for each library member and the background color represents the catalytic activity in terms of onset potential, as indicated by the scale bar. For ORR, the majority of the Pt-containing compositions showed better catalytic activity (less negative onset potential) than pure Pt (Figure 1a). Co−Mn binary compositions (with no Pt) did not exhibit high catalytic activity, but the addition of as little as 12% Pt to the system dramatically improved the activity of the catalyst. The best ORR catalyst from this system was $Pt_{12}Mn_{44}Co_{44}$, which had an onset potential of −78 mV vs SCE. This is an improvement of +142 mV over the standard onset potential of pure Pt (−220 mV), with the added benefit of lower Pt content, leading to a less expensive catalyst. This catalyst improves on results for reported Pt−Co alloy ORR catalysts in literature, which had onset potential of 160 mV vs SCE in alkaline solution.[39]

Results of the OER scans on Pt−Mn−Co libraries revealed somewhat similar trends in onset potential as compared to the ORR scans (Figure 1b). A wide range of Pt-containing alloys dramatically lowered the OER onset potential, and compositions near $Co_{50}Mn_{50}$ were reasonably active as well. Highly active compositions in this library performed slightly better than literature reports for polycrystalline Co, which has an OER onset potential of 540 mV vs SCE.[51] The composition with the

DOI: 10.1021/acscombsci.5b00030
ACS Comb. Sci. 2015, 17, 355−364

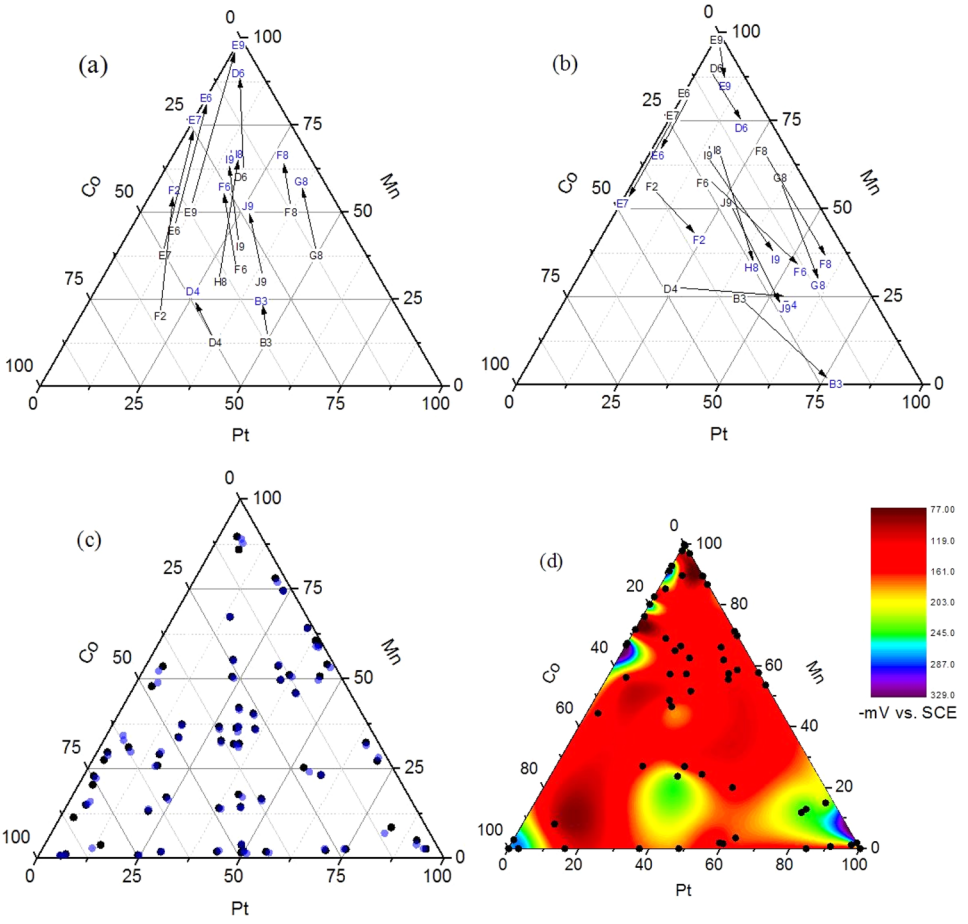

Figure 2. (a) Select compositions from the Pt−Mn−Co library contrasting bulk compositions (black) with surface compositions (blue) measured by XPS, demonstrating increased surface concentration of Mn. The alphanumeric symbols identify individual library members. (b) Surface compositions from the Pt−Mn−Co library before (black) and after (blue) electrochemical (EC) testing. (c) Bulk compositions of the Pt−Mn−Co library measured by XRF before (black) and after (blue) EC testing, showing virtually no change in overall composition. (d) ORR onset potentials for the Pt−Mn−Co library as a function of surface composition measured by XPS.

lowest OER onset potential was $Pt_{20}Co_{80}$ at 471 mV vs SCE, a decrease of 289 mV from Pt OER onset potential. The best ORR composition, $Pt_{12}Mn_{44}Co_{44}$, also catalyzed the OER very well, with onset potential of 539 mV vs SCE, a 221 mV decrease from Pt OER onset potential. This composition is therefore an excellent candidate as a bifunctional catalyst in a secondary Li−air battery, being able to effectively catalyze both the charge and discharge reactions.

Degradation evaluation of the Pt−Mn−Co system showed that Co-rich compositions tended to dissolve readily during the reaction, while most Pt-rich compositions were unaffected (Figure 1c). $Pt_{12}Mn_{44}Co_{44}$, the most active composition, showed discoloration but did not experience any spalling or edge loss. Further investigation would be needed to characterize the cause of the discoloration.

XRD characterization of the Pt−Mn−Co system showed that compositions exhibited the phases expected from the corresponding phase diagrams. Examples and discussion of this are available in the Supporting Information for this paper. The film surface composition of the entire Pt−Mn−Co library was examined using XPS measurements. This analysis revealed surface segregation of Mn in all library members which contained significant quantities of Mn. While XRF analysis of the same library confirmed the overall film compositions were as expected, the elevated Mn compositions in many XPS measurements suggested that a migration of Mn to the film surface took place during annealing. A selection of original compositions and the surface compositions determined by XPS are shown in Figure 2a. This phenomenon of Mn segregation has been previously observed during high- temperature annealing of sintered steels[52,53] and (Ga, Mn)As compounds,[54,55] but has not been encountered in Pt−Mn−Co ORR studies as other fabrication techniques do not utilize high-temperature annealing. Nørskov et al. showed that Pt and Mn have antisegregation tendencies at close-packed surfaces,[56] but in the present case Mn surface segregation appears to take place interstitially above temperatures of 180 °C.[54]

Comparisons of XPS and XRF measurements taken after the electrochemical test showed that Pt concentration increased and Mn concentration decreased at the surface of the combinatorial films while bulk composition remained relatively unaffected. The most likely explanation for this observation is that the Mn surface layer that forms during annealing is dissolved into the electrolyte during the electrochemical reaction, leaving a surface that is Mn-depleted compared to the bulk (Figure 2b) without affecting the overall composition of the film (Figure 2c). Plotting ORR catalytic activity against XPS-measured surface composition (Figure 2d) revealed no clear corresponding trend, suggesting that overall film composition and not postannealing surface composition is

DOI: 10.1021/acscombsci.5b00030
ACS Comb. Sci. 2015, 17, 355−364

the key variable determining catalytic activity in this case. For example, the most active bulk composition for ORR, $Pt_{12}Mn_{44}Co_{44}$, had a surface composition of $Mn_{83}Co_{17}$ after postdeposition annealing according to XPS measurements, with no Pt present at the surface. After the electrochemical test, the surface composition of this sample was $Pt_2Mn_{65}Co_{33}$. Other highly active samples with similar as-deposited compositions exhibited similar trends in surface composition change during electrochemical screening (Table 1). Literature reports exist of

Table 1. Surface Composition Changes during Electrochemical Screening for Similar Pt−Mn−Co Compositions

deposited composition	surface composition before screening	surface composition after screening
$Pt_{12}Mn_{44}Co_{44}$	$Mn_{83}Co_{17}$	$Pt_2Mn_{65}Co_{33}$
$Pt_{13}Mn_{37}Co_{50}$	$Mn_{77}Co_{23}$	$Pt_1Mn_{51}Co_{48}$
$Pt_{13}Mn_{50}Co_{37}$	$Mn_{98}Co_2$	$Pt_9Mn_{85}Co_6$

Mn−Co oxide spinels with similar compositions such as $Mn_{60}Co_{40}$[57] and $Mn_{75}Co_{25}$.[58] These compositions were both reported to have ORR onset potentials of ∼−200 mV vs SCE. The ORR onset potential of our $Pt_{12}Mn_{44}Co_{44}$ sample improves on this value by +122 mV. Hence the small amount of Pt is critical to the alloy catalytic activity.

Cr−Mn−Co. Pt was replaced with Cr to study non-noble metal catalyst materials, as several forms of Cr-based materials have been studied as electrocatalysts for ORR.[59−61] ORR onset potentials in this library were much lower than in the previous Pt−Mn−Co library, pointing to the catalytic effectiveness of Pt and its importance in alloys (Figure 3a). The highest ORR onset potential obtained in the Cr−Mn−Co library was for $Cr_{20}Mn_{20}Co_{60}$ at −262 mV vs SCE, 42 mV lower that Pt. While not as active as noble metal catalysts, it approaches the activity of Pt at a fraction of the cost.

Cr-rich ternary compositions showed significant reduction in OER onset potential compared to Pt (Figure 3b). The lowest OER onset potential was for $Cr_{66}Mn_{17}Co_{17}$ at 553 mV vs SCE, 207 mV lower than Pt. The composition with the highest ORR onset potential, $Cr_{20}Mn_{20}Co_{60}$, had an OER onset potential of 662 mV vs SCE, 98 mV lower than Pt. $Cr_{20}Mn_{20}Co_{60}$ showed some discoloration in the stability examination after testing, but no spalling took place after 10 cycles each of the ORR and OER scans (Figure 3c). On the basis of the assumption that ORR catalytic activity is more essential to battery performance, $Cr_{20}Mn_{20}Co_{60}$ is the most promising composition in this library, being slightly less effective as an ORR catalyst while offering mild improvement as an OER catalyst.

Pd−Mn−Co. Other metals were examined as possible replacements for Pt to improve catalytic activity over that seen in Cr−Mn−Co. Pd was examined as a lower-cost replacement for Pt because of its similar atomic structure and comparable ORR catalysis activity.[62] The Pd−Mn−Co library was constructed in the same way as previous libraries, including the Pt reference pads.

Unlike Pt in the Pt−Mn−Co library, not all Pd-containing compositions tested were highly active for ORR. Highly active compositions included $Pd_{12}Mn_{44}Co_{44}$, $Pd_{13}Mn_{50}Co_{37}$, $Pd_{60}Mn_{20}Co_{20}$, $Pd_{43}Co_{57}$, and $Pd_{80}Mn_{20}$, and were widely dispersed throughout the library (Figure 4a). Similar patterns were observed in the test for OER onset potential, where many of the same compositions that were active for ORR were active for OER as well (Figure 4b). In particular, compositions including more than 60% Co were highly active for OER. The Pd−Mn−Co library was robust in terms of the corrosion score ranking (Figure 4c). Only scores of 4 and 5 were assessed throughout the library, meaning that some compositions changed color after the electrochemical tests but there was no spalling or edge loss from any films.

The most promising composition discovered in the Pd−Mn−Co library was $Pd_{43}Co_{57}$. This composition had the highest ORR onset potential measured in the library at −111 mV vs SCE, which is an improvement of +109 mV over the Pt test pads and 33 mV lower than the best composition from the Pt−Mn−Co library, $Pt_{12}Mn_{44}Co_{44}$. $Pd_{43}Co_{57}$ also had the lowest OER onset potential in the Pd−Mn−Co library at 453 mV vs SCE, which is 307 mV lower than the Pt test pads and 18 mV lower than the best composition from the Pt−Mn−Co library, $Pt_{20}Co_{80}$. $Pd_{43}Co_{57}$ also scored 5 on the corrosion score test, meaning that the film was unchanged during the electrochemical reaction. All of these factors combine to make $Pd_{43}Co_{57}$ a promising composition for further study as a possible Li−air battery cathode catalyst.

XPS characterization of the surface and bulk compositions in the Pd−Mn−Co library after the annealing step (before EC test) revealed Mn surface segregation as with the Pt−Mn−Co library, but to a lesser extent (Figure 5a). The surface composition of $Pd_{43}Co_{57}$ was virtually identical to the bulk composition (point C3 in Figure 5a). However, a large amount of Mn dissolution from the surface took place during the EC

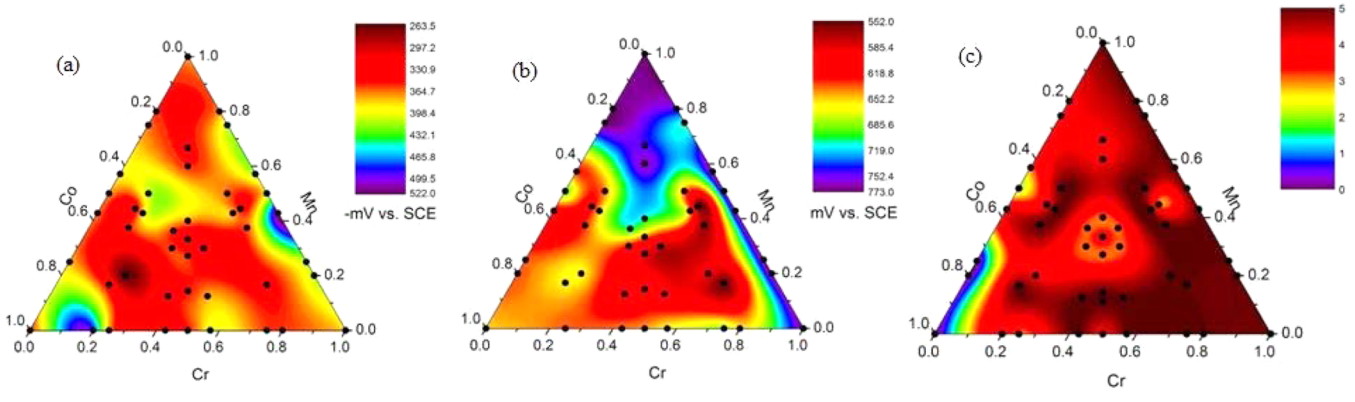

Figure 3. (a) ORR onset potential for the Cr−Mn−Co system. (b) OER onset potential for the Cr−Mn−Co system. (c) Corrosion scores for the Cr−Mn−Co system.

DOI: 10.1021/acscombsci.5b00030
ACS Comb. Sci. 2015, 17, 355−364

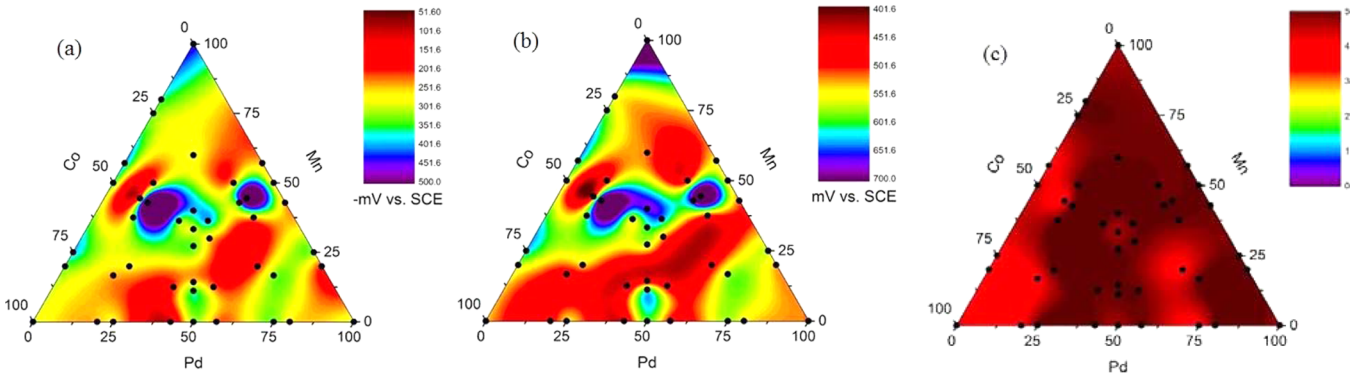

Figure 4. (a) ORR onset potential for the Pd−Mn−Co system. (b) OER onset potential for the Pd−Mn−Co system. (c) Corrosion scores for the Pd−Mn−Co system.

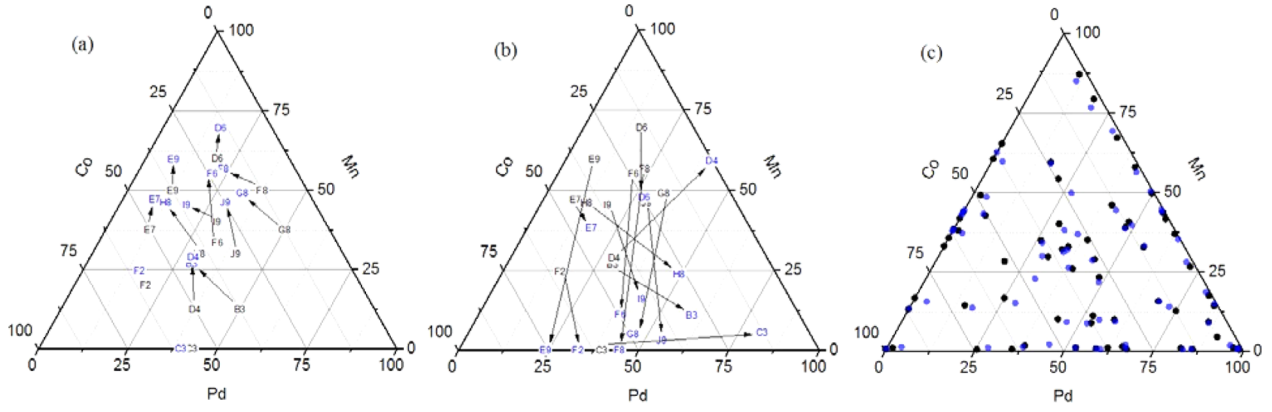

Figure 5. (a) Overall compositions (black) and surface compositions (blue) of select library members in the Pd−Mn−Co library. (b) Surface compositions of Pd−Mn−Co library members before (black) and after (blue) electrochemical screening. (c) Overall compositions of the Pd−Mn−Co library measured by XRF before (black) and after (blue) electrochemical screening.

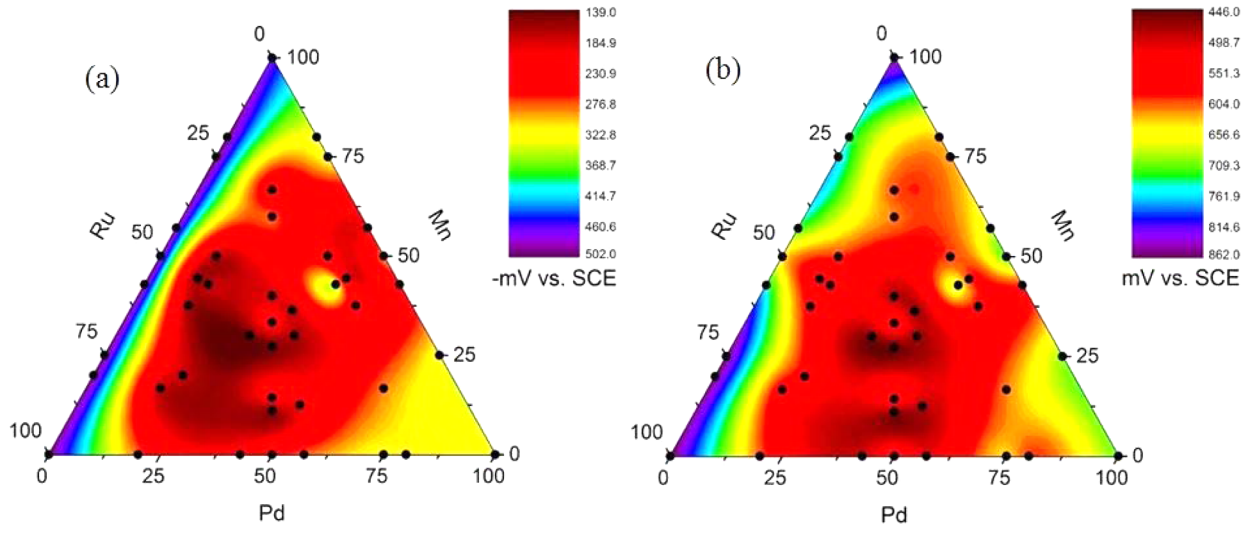

Figure 6. (a) ORR onset potential for the Pd−Mn−Ru system. (b) OER onset potential for the Pd−Mn−Ru system.

test (Figure 5b). Several compositions also showed Pd-enrichment at the surface, particularly $Pd_{43}Co_{57}$ (point C3), whose surface composition was $Pd_{82}Co_{18}$ after testing, suggesting that some leaching of near-surface Co occurred. XRF characterization before and after the EC test showed that bulk compositions were unchanged throughout the library. Surface dissolution was not significant enough to affect bulk composition (Figure 5c).

The most promising composition discovered in the Pd−Mn−Co library was $Pd_{43}Co_{57}$. This composition had the highest ORR onset potential measured in the library at −111 mV vs SCE, which is an improvement of +109 mV over the Pt test pads and 33 mV lower than the best composition from the Pt−Mn−Co library, $Pt_{12}Mn_{44}Co_{44}$. $Pd_{43}Co_{57}$ also had the lowest OER onset potential in the Pd−Mn−Co library at 453 mV vs SCE, which is 307 mV lower than the Pt test pads and

DOI: 10.1021/acscombsci.5b00030
ACS Comb. Sci. 2015, 17, 355−364

18 mV lower than the best composition from the Pt−Mn−Co library, $Pt_{20}Co_{80}$. $Pd_{43}Co_{57}$ also scored 5 on the corrosion score test, meaning that the film was unchanged during the electrochemical reaction. All of these factors combine to make $Pd_{43}Co_{57}$ a promising composition for further study as a possible Li−air battery cathode catalyst.

Pd−Mn−Ru. Ru is one of the best noble metal catalysts for OER and has been alloyed with Pt, Ir, and other noble metals in attempts to produce bifunctional catalysts.[63−66] Therefore, the library system Pd−Mn−Ru was fabricated and studied as a potential cathode catalyst. Binary combinations of manganese and ruthenium exhibited almost no catalytic activity for ORR, however adding as little as 11% palladium increased catalytic activity dramatically (Figure 6a). The compositions of greatest activity are near the center of the diagram, where electrodes contain roughly equal amounts of each material. The composition with the highest onset potential was $Pd_{36}Mn_{28}Ru_{36}$ at −137 mV vs SCE, a significant 83 mV higher than Pt. These results approach those obtained for the Pt−Mn−Co libraries, with the additional benefit of being Pt-free. Replacing Pt catalysts with Pd-containing catalysts would reduce the materials cost by approximately 1/3 based on current precious metals prices.

OER onset potentials followed the same trend as ORR onset potentials, which is promising for possible use as bifunctional catalysts (Figure 6b). The composition with the lowest OER onset potential was $Pd_{36}Mn_{28}Ru_{36}$ at 473 mV vs SCE, 287 mV lower than Pt. As a bifunctional catalyst, $Pd_{36}Mn_{28}Ru_{36}$ offered the best performance in the Pd−Mn−Ru system because its ORR onset potential (−146 mV vs SCE) was close to the highest activity while its OER onset potential was lower than all others by ∼20 mV. A catalyst stability diagram of this library is not shown because no degradation was observed for any composition. Mn surface composition levels were measured before and after electrochemical screening and showed similar patterns of Mn enrichment after thermal annealing followed by a Mn-poor surface after the electrochemical reaction as a result of near-surface Mn dissolution. Platinum is not recognized as an effective OER catalyst, and has previously been combined with gold to produce a bifunctional catalyst in a Li−air battery with an aprotic electrolyte.[11] $Pd_{36}Mn_{28}Ru_{36}$ has the potential to operate as an improved bifunctional catalyst in a Li−O_2 battery while providing less materials costs than a Pt−Au catalyst.

EXPERIMENTAL PROCEDURES

Magnetron sputtering was performed in a combinatorial sputtering system, which includes five sputtering guns in a sputter-up configuration in a stainless steel chamber. The chamber includes a moveable sample arm and a rotating carousel holding up to 12 shadow masks between the sputtering target and the substrate.[67] Sputtering targets were 2" in diameter and composed of metals of at least 99.99% purity. The sputtering chamber maintained a base vacuum pressure of 10^{-7} Torr, and a chamber pressure of 2 mTorr was commonly used for sputtering. Ar gas was introduced to the chamber at 20 sccm flow rate to strike the plasma. Gas mixtures of 25% N_2/75% Ar were also introduced through a second gas inlet for certain applications to perform reactive sputtering.

Sputtering rates were adjusted by varying the power (DC or RF) of the plasma, and deposition rates were determined ex situ using a quartz crystal oscillator. For a particular target material, sputtering was performed under identical conditions for different time periods on a set of four quartz crystal substrates. The change in oscillation frequency was then recorded and correlated to mass gain using the Sauerbrey Equation.[68]

Si wafers of 50 mm diameter were used as substrates for libraries. The wafers were first subjected to an RCA cleaning procedure, and then heated in an oxidation furnace to 1100 °C for 1 h under dry O_2, in order to grow a 1000 Å-thick SiO_2 layer on the Si surface. A layer of photoresist was applied to the wafer surface via spin coating and patterned into the electrical lead design using contact lithography. Next, TiN was reactively sputtered onto the wafer from a Ti target with N_2 reactive gas in the chamber, to a thickness of 2000 Å. The excess TiN film was then removed using a photolithographic liftoff process.

Ternary library deposition was accomplished by sputtering the three constituents from metallic targets through shadow masks onto the 76 hexagonal TiN current collection pads created by the liftoff. Thin layers approximately 25 Å thick were sputtered sequentially to form discrete thin film stacks on the TiN pads that consist of up to eight layers of each target material. The individual layer thicknesses were controlled to contain equimolar quantities of each material, so that the composition of each stack was controlled by the number of layers of each material present. For the typical library a set of six shadow masks was used (Supporting Information Figure S1), each of which exposes different electrode pads. The film stack composition was varied throughout the library by the specific sequence of masks through which the target materials were sputtered. The library recipe could be tuned to produce compositions in desired areas of the ternary system by altering the mask sequence and the number of layers of each material. A seventh mask was used to deposit a control material (usually Pt) on 12 electrode pads around the periphery of the library. A library consisted of 63 combinatorial electrodes, 12 Pt control electrodes, and one blank (TiN electrode) after sputtering was complete. After deposition, the library was annealed at 550 °C for fours under vacuum, followed by a rapid excursion to 900 °C for 5 min. Figure S2 in Supporting Information shows a completed library wafer.

Electrochemical testing was performed in a multichannel electrochemical cell connected to a Scribner multichannel microelectrode analyzer (MMA) potentiostat, shown schematically in Figure S3 in Supporting Information. The general design was adapted from one used in research on catalysts for direct methanol fuel cells.[69] The cell volume was defined by a 1.5 in. diameter quartz tube pressed against a Viton O-ring contacting the wafer surface. The O-ring was positioned so as to contain the electrolyte and not expose the electrical contact pads around the outside edge of the wafer to the electrolyte. Electrical contact was made to the MMA by pogo pins pressed against the peripheral contact pads. The interior of the cell was filled with electrolyte, and reference and counter electrodes were introduced from the top of the cell, as well as a gas diffusion bubbler. The reference electrode was a saturated calomel electrode (SCE) and the counter electrode was a Pt-coated Nb wire mesh ring. The electrolyte was aqueous 0.1 M KOH, which was selected based on the results of Crisotomo et al., who showed that trends observed in KOH testing were followed in Li−air battery experiments.[43]

The combinatorial library electrodes were screened for ORR catalytic activity using cyclic voltammetry. This allowed for the rapid screening of many samples in parallel, as each library pad functioned as an individual working electrode within the electrochemical cell. Initially, N_2 gas was bubbled through the

DOI: 10.1021/acscombsci.5b00030
ACS Comb. Sci. 2015, 17, 355−364

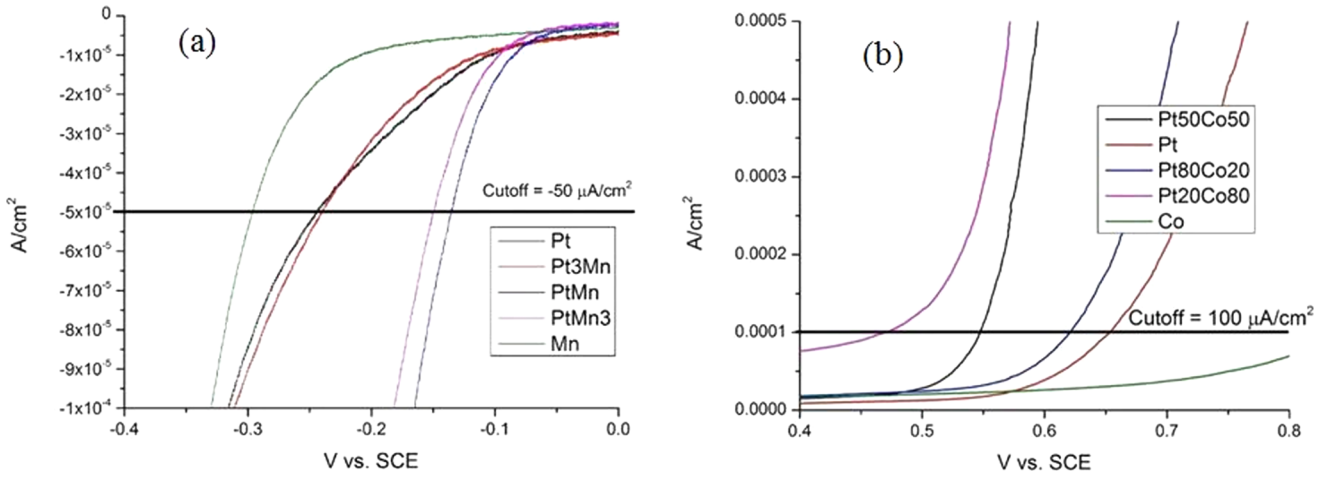

Figure 7. (a) Determination of ORR onset potential from Pt−Mn cyclic voltammograms. (b) Determination of OER onset potential from Pt−Co cyclic voltammograms.

Table 2. Summary of Catalytic Activity Results

library	best composition	ORR onset potential (mV vs SCE)	Pt-relative ORR (mV)	OER onset potential (mV vs SCE)	Pt-relative OER (mV)
Pt−Mn−Co	$Pt_{12}Mn_{44}Co_{44}$	−78	+142	539	−221
Cr−Mn−Co	$Cr_{20}Mn_{20}Co_{60}$	−262	−42	662	−98
Pd−Mn−Co	$Pd_{43}Co_{57}$	−111	+109	453	−307
Pd−Mn−Ru	$Pd_{36}Mn_{28}Ru_{36}$	−146	+74	473	−287

electrolyte for 30 min while the cell was held at open circuit voltage (OCV). The cell potential was then cycled between 0.2 and −0.8 V vs SCE at a scan rate of 10 mV/s until the cyclic voltammograms stabilized, which usually occurred within 10 cycles. The electrolyte was then bubbled with O_2 for 30 min while the cell was held at OCV after which the same set of potential scans was repeated. Libraries were also tested for OER catalytic activity by cycling the cell potential between −0.2 and 0.8 V vs SCE at a scan rate of 10 mV/s for a total of 10 cycles.

Library compositions were ranked according to the onset potential of the ORR during the anodic scan. By examining the initiation of ORR during the oxygen voltammogram, the onset potential was defined as the potential at which the current density for each electrode passed −50 μA/cm^2. This value was found to be greater than the exchange current density of the nitrogen voltammogram, but very near the potential at which ORR began to occur (Figure 7a). The ORR onset potential of Pt is ∼−220 mV vs SCE, with more positive onset potentials associated with a particular electrode composition representing improved catalytic activity. Similarly, compositions were ranked according to the onset potential of the OER during the cathodic scan, with more negative onset potentials representing improvements in OER catalytic activity. Examining the OER voltammograms in the same method as the ORR scans, the OER onset potential was defined as the potential at which the current passed 100 μA/cm^2, and is ∼760 mV vs SCE for Pt electrodes (Figure 7b).

Optical micrographs were taken of each library wafer before and after electrochemical testing in order to visually document any film degradation as a result of testing. Compositions were qualitatively ranked for durability on a scale of 0−5 based on the level of visible corrosion after electrochemical testing (Supporting Information Table S1 and Figure S4). A score of 5 corresponded to no change after testing, while 4 denoted only a change in color. A score of 3 signified spalling of the film, while 2 was for observed edge loss. A score of 1 represented both spalling and edge loss, and compositions received a score of 0 if the combinatorial film had vanished entirely, leaving only the bare TiN electrode pad.

A Scintag X1 powder X-ray diffractometer (XRD) was used to characterize the phases present in the combinatorial electrodes before electrochemical testing was conducted. An EVO 50 Zeiss scanning electron microscope (SEM) equipped with an Inca X-Sight energy dispersive X-ray spectroscopy (EDS) detector was used to study film surface microstructure and confirm film composition and homogeneity. Film compositions were studied further using an Edax Orbis X-ray fluorescence (XRF) instrument and a PHI VersaProbe II X-ray photoelectron spectrometer (XPS).

■ CONCLUSION

A combinatorial library synthesis and high throughput screening process for the discovery of Li−air battery cathode materials has been reported. Thin-film catalyst materials were deposited by sputter deposition into a discrete ternary composition library. They were then tested for catalytic activity toward the ORR and OER in parallel using cyclic voltammetry in alkaline media and ranked according to onset potential with respect to Pt. with By this approach the composition variation between samples is the only factor influencing differences in catalytic activity for ORR and OER, allowing entire ternary metal alloy composition systems to be efficiently examined. Results from the Pt−Mn−Co, Cr−Mn−Co, Pd−Mn−Co, and Pd−Mn−Ru libraries were reported.

Catalytic activity results of the best overall compositions from the libraries tested are summarized in Table 2. In terms of ORR catalytic activity, $Pt_{12}Mn_{44}Co_{44}$ exhibited the highest activity, improving significantly on the performance of pure Pt. The ORR onset potentials of $Pd_{43}Co_{57}$ and $Pd_{36}Mn_{28}Ru_{36}$ showed large improvements over pure Pt as well, while $Pd_{43}Co_{57}$ was the top performer for OER catalytic activity.

DOI: 10.1021/acscombsci.5b00030
ACS Comb. Sci. 2015, 17, 355−364

These alloys show great promise as Pt-free catalysts, although the high cost of Pd still renders them fairly expensive. $Cr_{20}Mn_{20}Co_{60}$ is contrastingly much less expensive, and while not quite as active as Pt for ORR did perform slightly better than Pt for OER.

The thin film combinatorial evaluation is only a first level screening of potential catalyst compositions, however. More research on potential compositions identified by this method is required in the form that the catalysts would ultimately be applied (e.g., as powder on a catalyst support) to confirm activity. Finally, such catalysts also need to be cycled in Li−O_2 battery test cells to confirm voltage and capacity performance, as well as durability.

■ ASSOCIATED CONTENT

Supporting Information

Schematics of combinatorial sputtering process and homemade high-throughput electrochemical cell, examples of optical screening of library members for durability, and examples of library member characterization by X-ray diffraction. The Supporting Information is available free of charge on the ACS Publications website at DOI: 10.1021/acscombsci.5b00030.

■ AUTHOR INFORMATION

Corresponding Author

*E-mail: pmcginn@nd.edu.

Notes

The authors declare no competing financial interest.

■ ACKNOWLEDGMENTS

The authors gratefully acknowledge funding from the U.S. Army TARDEC under Contract No. W56HZV-08-C-0236, through a subcontract with Mississippi State University. Any opinions, findings, and conclusions or recommendations expressed in this material are those of the authors and do not necessarily reflect the views of the U.S. Army TARDEC. We thank the Center for Sustainable Energy at Notre Dame (cSEND) Materials Characterization Facilities for the use of the PHI VersaProbe II X-ray Photoelectron Spectrometer. We acknowledge support of the National Science Foundation through MRI award 1126374 for the XPS data in this paper.

■ ABBREVIATIONS

ORR, oxygen reduction reaction; OER, oxygen evolution reaction; OCV, open circuit voltage; SCE, saturated calomel electrode; XRD, X-ray diffraction; SEM, scanning electron microscope; EDS, energy-dispersive X-ray spectroscopy; XRF, X-ray fluorescence; XPS, X-ray photoelectron spectroscopy

■ REFERENCES

(1) Goodenough, J. B.; Kim, Y. Challenges for Rechargeable Li Batteries. *Chem. Mater.* **2010**, *22* (3), 587−603.
(2) Freunberger, S. A.; Chen, Y.; Peng, Z.; Griffin, J. M.; Hardwick, L. J.; Bardé, F.; Novák, P.; Bruce, P. G. Reactions in the Rechargeable Lithium−O_2 Battery with Alkyl Carbonate Electrolytes. *J. Am. Chem. Soc.* **2011**, *133* (20), 8040−8047.
(3) Armand, M.; Tarascon, J.-M. Building Better Batteries. *Nature* **2008**, *451*, 652−657.
(4) Abraham, K. M.; Jiang, Z. A Polymer Electrolyte-Based Rechargeable Lithium/Oxygen Battery. *J. Electrochem. Soc.* **1996**, *143* (1), 1−5.
(5) Rahman, M. A.; Wang, X.; Wen, C. A Review of High Energy Density Lithium−Air Battery Technology. *J. Appl. Electrochem.* **2013**, *44* (1), 5−22.
(6) Dunn, B.; Kamath, H.; Tarascon, J.-M. Electrical Energy Storage for the Grid: A Battery of Choices. *Science* **2011**, *334* (6058), 928−935.
(7) Woo, S.; Kim, I.; Lee, J. K.; Bong, S.; Lee, J.; Kim, H. Preparation of Cost-Effective Pt−Co Electrodes by Pulse Electrodeposition for PEMFC Electrocatalysts. *Electrochim. Acta* **2011**, *56* (8), 3036−3041.
(8) Christensen, J.; Albertus, P.; Sanchez-Carrera, R. S.; Lohmann, T.; Kozinsky, B.; Liedtke, R.; Ahmed, J.; Kojic, A. A Critical Review of Li/Air Batteries. *J. Electrochem. Soc.* **2011**, *159* (2), R1−R30.
(9) Ren, X.; Zhang, S. S.; Tran, D. T.; Read, J. Oxygen Reduction Reaction Catalyst on Lithium/air Battery Discharge Performance. *J. Mater. Chem.* **2011**, *21* (27), 10118−10125.
(10) Chen, J.; Cheng, F. Metal−Air Batteries: From Oxygen Reduction Electrochemistry to Cathode Catalysts. *Chem. Soc. Rev.* **2012**, *41* (6), 2172−2192.
(11) Lu, Y.-C.; Xu, Z.; Gasteiger, H. A.; Chen, S.; Hamad-Schifferli, K.; Shao-Horn, Y. Platinum−Gold Nanoparticles: A Highly Active Bifunctional Electrocatalyst for Rechargeable Lithium−Air Batteries. *J. Am. Chem. Soc.* **2010**, *132* (35), 12170−12171.
(12) Beattie, S. D.; Manolescu, D. M.; Blair, S. L. High-Capacity Lithium−Air Cathodes. *J. Electrochem. Soc.* **2009**, *156* (1), A44−A47.
(13) Li, Y.; Wang, J.; Li, X.; Liu, J.; Geng, D.; Yang, J.; Li, R.; Sun, X. Nitrogen-Doped Carbon Nanotubes as Cathode for Lithium−Air Batteries. *Electrochem. Commun.* **2011**, *13* (7), 668−672.
(14) Sammes, N.; Yamamoto, O.; Takeda, Y.; Hirano, A.; Shimonishi, Y.; Zhang, T.; Imanishi, N. A Novel High Energy Density Rechargeable Lithium/air Battery. *Chem. Commun.* **2010**, *46* (10), 1661−1663.
(15) Lu, Y.-C.; Gasteiger, H. a.; Crumlin, E.; McGuire, R.; Shao-Horn, Y. Electrocatalytic Activity Studies of Select Metal Surfaces and Implications in Li−Air Batteries. *J. Electrochem. Soc.* **2010**, *157* (9), 1016.
(16) Débart, A.; Paterson, A. J.; Bao, J.; Bruce, P. G. Alpha-MnO_2 Nanowires: A Catalyst for the O_2 Electrode in Rechargeable Lithium Batteries. *Angew. Chem.* **2008**, *47* (24), 4521−4524.
(17) Cheng, H.; Scott, K. Carbon-Supported Manganese Oxide Nanocatalysts for Rechargeable Lithium−Air Batteries. *J. Power Sources* **2010**, *195* (5), 1370−1374.
(18) Débart, A.; Bao, J.; Armstrong, G.; Bruce, P. G. An O_2 Cathode for Rechargeable Lithium Batteries: The Effect of a Catalyst. *J. Power Sources* **2007**, *174* (2), 1177−1182.
(19) Nikolova, V.; Iliev, P.; Petrov, K.; Vitanov, T.; Zhecheva, E.; Stoyanova, R.; Valov, I.; Stoychev, D. Electrocatalysts for Bifunctional Oxygen/air Electrodes. *J. Power Sources* **2008**, *185* (2), 727−733.
(20) Suntivich, J.; May, K. J.; Gasteiger, H. A.; Goodenough, J. B.; Shao-Horn, Y. A Perovskite Oxide Optimized for Oxygen Evolution Catalysis from Molecular Orbital Principles. *Science* **2011**, *334* (6061), 1383−1385.
(21) Lima, F. H. B.; Zhang, J.; Shao, M. H.; Sasaki, K.; Vukmirovic, M. B.; Ticianelli, E. A.; Adzic, R. R. Catalytic Activity−d-Band Center Correlation for the O_2 Reduction Reaction on Platinum in Alkaline Solutions. *J. Phys. Chem. C* **2007**, *111* (1), 404−410.
(22) Stamenkovic, V. R.; Fowler, B.; Mun, B. S.; Wang, G.; Ross, P. N.; Lucas, C. A.; Marković, N. M. Improved Oxygen Reduction Activity on $Pt_3Ni(111)$ via Increased Surface Site Availability. *Science* **2007**, *315* (5811), 493−497.
(23) Maier, W. F.; Stöwe, K.; Sieg, S. Combinatorial and High-Throughput Materials Science. *Angew. Chem., Int. Ed.* **2007**, *46* (32), 6016−6067.
(24) Potyrailo, R.; Rajan, K.; Stoewe, K.; Takeuchi, I.; Chisholm, B.; Lam, H. Combinatorial and High-Throughput Screening of Materials Libraries: Review of State of the Art. *ACS Comb. Sci.* **2011**, *13* (6), 579−633.
(25) Muster, T. H.; Trinchi, A.; Markley, T. A.; Lau, D.; Martin, P.; Bradbury, A.; Bendavid, A.; Dligatch, S. A Review of High Throughput

DOI: 10.1021/acscombsci.5b00030
ACS Comb. Sci. 2015, 17, 355−364

and Combinatorial Electrochemistry. *Electrochim. Acta* **2011**, *56* (27), 9679−9699.
(26) Todd, A. D. W.; Ferguson, P. P.; Fleischauer, M. D.; Dahn, J. R. Tin-Based Materials as Negative Electrodes for Li-Ion Batteries: Combinatorial Approaches and Mechanical Methods. *Int. J. Energy Res.* **2010**, *34* (6), 535−555.
(27) Spong, A. D.; Vitins, G.; Guerin, S.; Hayden, B. E.; Russell, A. E.; Owen, J. R. Combinatorial Arrays and Parallel Screening for Positive Electrode Discovery. *J. Power Sources* **2003**, *119*−*121* (0), 778−783.
(28) Roberts, M. R.; Vitins, G.; Denuault, G.; Owen, J. R. High Throughput Electrochemical Observation of Structural Phase Changes in $LiFe_{1-x}Mn_xPO_4$ during Charge and Discharge. *J. Electrochem. Soc.* **2010**, *157* (4), A381−A386.
(29) Fujimoto, K.; Takada, K.; Sasaki, T.; Watanabe, M. Combinatorial Approach for Powder Preparation of Pseudo-Ternary System $LiO_{0.5}$−X−TiO_2 (X: $FeO_{1.5}$, $CrO_{1.5}$ and NiO). *Appl. Surf. Sci.* **2004**, *223* (1−3), 49−53.
(30) Takada, K.; Fujimoto, K.; Sasaki, T.; Watanabe, M. Combinatorial Electrode Array for High-Throughput Evaluation of Combinatorial Library for Electrode Materials. *Appl. Surf. Sci.* **2004**, *223* (1−3), 210−213.
(31) Jiang, R.; Chu, D. An Electrode Probe for High-Throughput Screening of Electrochemical Libraries. *Rev. Sci. Instrum.* **2005**, *76* (6), 062213.
(32) Jiang, R. Combinatorial Electrochemical Cell Array for High Throughput Screening of Micro-Fuel-Cells and Metal/Air Batteries. *Rev. Sci. Instrum.* **2007**, *78* (7), No. 072209.
(33) Whitacre, J. F.; West, W. C.; Ratnakumar, B. V. A Combinatorial Study of $Li_yMn_xNi_{2-x}O_4$ Cathode Materials Using Microfabricated Solid-State Electrochemical Cells. *J. Electrochem. Soc.* **2003**, *150* (12), A1676−A1683.
(34) Jun, Y. J.; Park, S. H.; Woo, S. I. Combinatorial High-Throughput Optical Screening of High Performance Pd Alloy Cathode for Hybrid Li−Air Battery. *ACS Comb. Sci.* **2014**, *16* (12), 670−677.
(35) Girishkumar, G.; McCloskey, B.; Luntz, A. C.; Swanson, S.; Wilcke, W. Lithium−Air Battery: Promise and Challenges. *J. Phys. Chem. Lett.* **2010**, *1* (14), 2193−2203.
(36) McCloskey, B. D.; Bethune, D. S.; Shelby, R. M.; Girishkumar, G.; Luntz, A. C. Solvents' Critical Role in Nonaqueous Lithium−Oxygen Battery Electrochemistry. *J. Phys. Chem. Lett.* **2011**, *2* (10), 1161−1166.
(37) Kiros, Y. Electrocatalytic Properties of Co, Pt, and Pt−Co on Carbon for the Reduction of Oxygen in Alkaline Fuel Cells. *J. Electrochem. Soc.* **1996**, *143* (7), 2152−2157.
(38) Perez, J.; Gonzalez, E. R.; Ticianelli, E. A. Oxygen Electrocatalysis on Thin Porous Coating Rotating Platinum Electrodes. *Electrochim. Acta* **1998**, *44* (8−9), 1329−1339.
(39) Lima, F. H. B.; Ticianelli, E. A. Oxygen Electrocatalysis on Ultra-Thin Porous Coating Rotating Ring/disk Platinum and Platinum−Cobalt Electrodes in Alkaline Media. *Electrochim. Acta* **2004**, *49* (24), 4091−4099.
(40) Duong, H. T.; Rigsby, M. A.; Zhou, W.-P.; Wieckowski, A. Oxygen Reduction Catalysis of the Pt_3Co Alloy in Alkaline and Acidic Media Studied by X-Ray Photoelectron Spectroscopy and Electrochemical Methods. *J. Phys. Chem. C* **2007**, *111* (36), 13460−13465.
(41) Jiang, S.; Ma, Y.; Jian, G.; Tao, H.; Wang, X.; Fan, Y.; Lu, Y.; Hu, Z.; Chen, Y. Facile Construction of Pt−Co/CN_x Nanotube Electrocatalysts and Their Application to the Oxygen Reduction Reaction. *Adv. Mater.* **2009**, *21* (48), 4953−4956.
(42) Mao, L.; Zhang, D.; Sotomura, T.; Nakatsu, K.; Koshiba, N.; Ohsaka, T. Mechanistic Study of the Reduction of Oxygen in Air Electrode with Manganese Oxides as Electrocatalysts. *Electrochim. Acta* **2003**, *48* (8), 1015−1021.
(43) Crisostomo, V. M. B.; Ngala, J. K.; Alia, S.; Dobley, A.; Morein, C.; Chen, C.-H.; Shen, X.; Suib, S. L. New Synthetic Route, Characterization, and Electrocatalytic Activity of Nanosized Manganite. *Chem. Mater.* **2007**, *19* (7), 1832−1839.
(44) Xiang, X.-D.; Sun, X.; Briceño, G.; Lou, Y.; Wang, K.-A.; Chang, H.; Wallace-Freedman, W. G.; Chen, S.-W.; Schultz, P. G. A Combinatorial Approach to Materials Discovery. *Science* **1995**, *268* (5218), 1738−1740.
(45) Wieckowski, A.; Spendelow, J. S. Electrocatalysis of Oxygen Reduction and Small Alcohol Oxidation in Alkaline Media. *Phys. Chem. Chem. Phys.* **2007**, *9* (21), 2654−2675.
(46) Shim, J. H.; Kim, Y. S.; Kang, M.; Lee, C.; Lee, Y. Electrocatalytic Activity of Nanoporous Pd and Pt: Effect of Structural Features. *Phys. Chem. Chem. Phys.* **2012**, *14* (11), 3974−3979.
(47) Birss, V. I.; Damjanovic, A.; Hudson, P. G. Oxygen Evolution at Platinum Electrodes in Alkaline Solutions: II. Mechanism of the Reaction. *J. Electrochem. Soc.* **1986**, *133* (8), 1621−1625.
(48) Bonakdarpour, A.; Stevens, K.; Vernstrom, G. D.; Atanasoski, R.; Schmoeckel, A. K.; Debe, M. K.; Dahn, J. R. Oxygen Reduction Activity of Pt and Pt−Mn−Co Electrocatalysts Sputtered on Nano-Structured Thin Film Support. *Electrochim. Acta* **2007**, *53* (2), 688−694.
(49) Ahluwalia, R. K.; Wang, X.; Lajunen, A.; Steinbach, A. J.; Hendricks, S. M.; Kurkowski, M. J.; Debe, M. K. Kinetics of Oxygen Reduction Reaction on Nanostructured Thin-Film Platinum Alloy Catalyst. *J. Power Sources* **2012**, *215*, 77−88.
(50) Ammam, M.; Easton, E. B. Ternary PtMnX/C (X = Fe, Co, Ni, Cu, Mo and Sn) Alloy Catalysts for Ethanol Electrooxidation. *J. Electrochem. Soc.* **2012**, *159* (5), B635−B640.
(51) Lyons, M. E. G.; Brandon, M. P. The Oxygen Evolution Reaction on Passive Oxide Covered Transition Metal Electrodes in Alkaline Solution. Part 2-Cobalt. *Int. J. Electrochem. Sci.* **2008**, *3* (12), 1425−1462.
(52) Šalak, A.; Selecká, M. Effect of Manganese Content and Manganese Carrier on Properties of Sintered and Sinter Hardened Hybrid Fe−3Cr−0.5Mo−*x*Mn−0.24C Steel. *Powder Metall.* **2008**, *51* (4), 327−339.
(53) Rosso, M.; Kabátová, M.; Bidulský, R.; Hryha, E.; Grande, M. A.; Dudrová, E. Improvement of Mechanical Properties of Fe−Cr−Mo−[Cu−Ni]−C Sintered Sintered Steels by Sinter Hardening. *Mater. Sci. Forum* **2011**, *672*, 31−38.
(54) Edmonds, K.; Boguslawski, P.; Wang, K.; Campion, R.; Novikov, S.; Farley, N.; Gallagher, B.; Foxon, C.; Sawicki, M.; Dietl, T.; Nardelli, M. B.; Bernholc, J. Mn Interstitial Diffusion in (Ga,Mn)As. *Phys. Rev. Lett.* **2004**, *92* (3), No. 037201.
(55) Schmid, B.; Müller, A.; Sing, M.; Claessen, R.; Wenisch, J.; Gould, C.; Brunner, K.; Molenkamp, L.; Drube, W. Surface Segregation of Interstitial Manganese in $Ga_{1-x}Mn_xAs$ Studied by Hard X-Ray Photoemission Spectroscopy. *Phys. Rev. B* **2008**, *78* (7), No. 075319.
(56) Ruban, A. V.; Skriver, H. L.; Nørskov, J. K. Surface Segregation Energies in Transition-Metal Alloys. *Phys. Rev. B: Condens. Matter Mater. Phys.* **1999**, *59* (24), 15990−16000.
(57) Ohno, M.; Sugawara, M.; Matsuki, K. Oxygen Reduction Catalysis of Mn−Co Spinel Oxides on Agraphite Electrode in Alkaline Solution. *J. Mater. Chem.* **1997**, *7* (5), 833−836.
(58) Queiroz, A. C.; Lima, F. H. B. Electrocatalytic Activity and Stability of Co- and Mn-Based Oxides for the Oxygen Reduction Reaction in Alkaline Electrolyte. *J. Electroanal. Chem.* **2013**, *707*, 142−150.
(59) Mukerjee, S. Reviews of Applied Electrochemistry 0.23. Particle-Size and Structural Effects in Platinum Electrocatalysis. *J. Appl. Electrochem.* **1990**, *20* (4), 537−548.
(60) Stonehart, P. Development of Alloy Electrocatalysts for Phosphoric-Acid Fuel-Cells (PAFC). *J. Appl. Electrochem.* **1992**, *22* (11), 995−1001.
(61) Freund, A.; Lang, J.; Lehmann, T.; Starz, K. A. Improved Pt Alloy Catalysts for Fuel Cells. *Catal. Today* **1996**, *27* (1−2), 279−283.
(62) Suo, Y.; Zhuang, L.; Lu, J. First-Principles Considerations in the Design of Pd-Alloy Catalysts for Oxygen Reduction. *Angew. Chem., Int. Ed.* **2007**, *46* (16), 2862−2864.
(63) Miles, M. H.; Klaus, E. A.; Gunn, B. P.; Locker, J. R.; Serafin, W. E.; Srinivasan, S. The Oxygen Evolution Reaction on Platinum,

DOI: 10.1021/acscombsci.5b00030
ACS Comb. Sci. 2015, 17, 355−364

Iridium, Ruthenium and Their Alloys at 80 °C in Acid Solutions. *Electrochim. Acta* **1978**, *23* (6), 521−526.
(64) Chen, G.; Delafuente, D. A.; Sarangapani, S.; Mallouk, T. E. Combinatorial Discovery of Bifunctional Oxygen Reduction—Water Oxidation Electrocatalysts for Regenerative Fuel Cells. *Catal. Today* **2001**, *67* (4), 341−355.
(65) Yu, E. H.; Scott, K.; Reeve, R. W. Electrochemical Reduction of Oxygen on Carbon Supported Pt and Pt/Ru Fuel Cell Electrodes in Alkaline Solutions. *Fuel Cells* **2003**, *3* (4), 169−176.
(66) Rivas, S.; Arriaga, L. G.; Morales, L.; Fernandez, A. M. Evaluation of Pt−Ru−Ir as Bifunctional Electrocatalysts for the Oxygen Electrode in a Unitized Regenerative Fuel Cell. *Int. J. Electrochem. Sci.* **2012**, *7* (4), 3601−3609.
(67) Cooper, J. S.; Zhang, G.; McGinn, P. J. Plasma Sputtering System for Deposition of Thin Film Combinatorial Libraries. *Rev. Sci. Instrum.* **2005**, *76* (6), No. 062221.
(68) Sauerbrey, G. Verwendung von Schwingquarzen Zur Wagung Dunner Schichten Und Zur Mikrowagung. *Z. Med. Phys.* **1959**, 206−222.
(69) Cooper, J. S.; McGinn, P. J. Combinatorial Screening of Thin Film Electrocatalysts for a Direct Methanol Fuel Cell Anode. *J. Power Sources* **2006**, *163* (1), 330−338.

DOI: 10.1021/acscombsci.5b00030
ACS Comb. Sci. 2015, 17, 355−364